

## Self-consistent predictive modelling of 15 MA inductive scenarios in ITER

F. Koechl<sup>1</sup>, V. Parail<sup>2</sup>, M. Mattei<sup>3</sup>, R. Ambrosino<sup>4</sup>, G. Corrigan<sup>2</sup>, L. Garzotti<sup>2</sup>, C. Labate<sup>5</sup>,  
D. C. McDonald<sup>2</sup>, G. Saibene<sup>6</sup>, R. Sartori<sup>6</sup> and JET EFDA contributors<sup>\*</sup>

*JET-EFDA, Culham Science Centre, OX14 3DB, Abingdon, UK; <sup>1</sup>Association EURATOM-ÖAW/ATI, Atominstitut, TU Wien, 1020 Vienna, Austria; <sup>2</sup>Association EURATOM-CCFE Fusion Association, Culham Science Centre, Abingdon, UK; <sup>3</sup>Association EURATOM-ENEA-CREATE, Seconda University di Napoli, Aversa (CE), Italy; <sup>4</sup>Association EURATOM-ENEA-CREATE, Università di Napoli Parthenope, Napoli (NA), Italy; <sup>5</sup>Association EURATOM-ENEA-CREATE, Università di Reggio Calabria, Italy; <sup>6</sup>Fusion for Energy, Barcelona, Spain.*

**Introduction:** Integrated simulations combining the free boundary equilibrium code CREATE-NL [1] and the JET suite of codes JINTRAC [2] have been performed for the prediction of the 15 MA ELMMy H-mode scenario in ITER in order to assess its viability, its operational space, its compatibility with machine constraints, in particular with the poloidal field (PF) coil system, and to evaluate possible risks related to transient events as e.g. an H-L transition. To this end, an analysis of the sensitivity of the scenario to the current ramp rate  $dI_{pl}/dt$ , to heating and fuelling schemes, to the time of transitions to (L-H) and from (H-L) H-mode, to the dynamic of these transitions and to the assumptions on the H-mode evolution from the L-H transition to  $Q = 10$  has been done. The results of these sensitivity studies and their consequences on the scenario are the subject of this paper.

**Simulation conditions and results:** The agreement of the plasma shape with the desired target shape evolution is evaluated at reference gaps and maintained by application of PF coil feedback correction currents on top of pre-programmed nominal currents. For the prediction of the plasma core evolution, fully (including density) and semi-predictive (prescribed density) simulations were performed, solving the particle diffusion transport equation by assumption of a continuous pellet source and zero recycling in the first case and prescribing density profiles with a given fraction of Greenwald density  $n_G$  in the latter. The anomalous transport models Bohm/gyroBohm [3] for L-mode and GLF-23 [4] for H-mode in combination with an ETB model emulating time-averaged ELMs [5] have been applied. Information about the plasma and equilibrium states is exchanged in a self-consistent way between the codes. A reference scenario was defined with heating and fuelling conditions as summarised in tables 1-2. Durations for the ramp-up, flat-top and ramp-down phases for the reference scenario of 80 s, 450 s and 200 s resp. were assumed in compliance with the requirement that enough margin should be left regarding headroom of the PF coil system for the transient phases. Voltsecond consumption was determined following the axial method described in [6].

*Sensitivity to timing of the L-H transition:* An anticipated transition to H-mode during current ramp-up helps to reduce Vs consumption. It may reduce the risk of low-frequency NTM-triggering sawteeth by reduction of the radial position of  $q = 1$  [7] and facilitate plasma control after the transition due to reduced alpha heating at lower currents. However, the ratio  $s/q$  between shear and safety factor decreases in the early phase of flat-top, causing an amplification of microturbulences in the core according to experimental observations [8] and predictions with GLF-23 as detailed in [9,10] and a reduction in fusion performance by up to  $\approx 60\%$  (see figure 2).

*Optimisation of the plasma current ramp-up and ramp-down and sensitivity to the plasma current ramp rate:* A sensitivity scan for the ramp-up phase was performed with respect to  $dI_{pl}/dt$ , the amount of auxiliary heating, the density level and boundary conditions. For higher ramp rates and off-axis heating power, lower values for the internal inductance  $li(3)$  and a reduction in Vs consumption can be achieved (see figure 1). Plasma profiles at the end of ramp-up are insensitive to assumptions for fuelling and boundary conditions. If the current is ramped up at the maximum rate that can be provided by the PF coil system, the flat-top performance is degraded compared to the reference scenario for the same reasons that cause a degradation for an early L-H transition. In the current ramp-down, the application of the maximum available current ramp rate helps to improve the Vs balance, but plasma control related to vertical stability and density pump-out becomes more demanding ( $\rightarrow$  figures 3-4). Some of these conclusions have been confirmed in the experiment [11]. The effect of

<sup>\*</sup> See the Appendix of F. Romanelli et al., Proceedings of the 23rd IAEA FEC 2010, Daejeon, Korea

a variation in ramp rate on  $I_{\text{li}}(3)$  and  $V_s$  for the current ramp-down phase is shown in figure 5. Resistive current losses are dominant in the late phase of ramp-down due to the decrease in temperature. With a late divertor-limiter phase transition, high  $P_{\text{AUX}}$  can be maintained at lower  $I_{\text{pl}}$  which helps to shape the current profile and reduce resistive losses. Sawtooth-induced  $V_s$  consumption plays a role in the early phase after the H-L transition, as  $q$  scales inversely with plasma current.

*Sensitivity to H-L transition dynamic:* A scan in the foreseeable thermal energy decrease rate  $dW_{\text{th}}/dt$  after the H-L transition, depending on possible transitional plasma confinement states like a type-III ELM regime, the speed of the reduction in fusion power  $P_{\text{fus}}$ , the alpha particle thermalisation and energy confinement times and the level of  $P_{\text{AUX}}$  reduction, was carried out and the most extreme case with the maximum conceivable  $dW_{\text{th}}/dt$  has been determined. From the point of view of plasma control, the requirement is that the plasma cannot touch the inner wall even in case of an unanticipated plasma transition. According to first simulation results applying linear models for the calculation of PF coil feedback control currents, the plasma position can be controlled if it is kept at a distance of more than 20 cm from the inner wall before the onset of the H-L transition (→ figure 6, cf. [12]). Plasma control can also be maintained for the maximum ramp rate scenario. However, in this and other realisations of the transition the system can be pushed towards its controllability limits as the safety specifications in terms of minimum plasma wall clearance cannot always be met.

*Sensitivity to timing of the H-L transition:* In order to reduce resistive and sawtooth-induced  $V_s$  losses, it is highly preferable to maintain H-mode conditions during ramp-down for as long as possible. The current ramp-down period could then be considerably enhanced to more than 400 s. With the help of alpha particle heating in the early phase of ramp-down and strong auxiliary heating later on, it appears to be possible to delay the H-L transition until a current level of 7 MA (→ figures 7-8). This result was confirmed in semi-predictive simulations for density levels in a range of 40-80% of  $n_G$ .

*Self-consistent simulations of the plasma evolution after the L-H / H-L transition:* Fully predictive simulations of self-consistent transitions to and from H-mode applying a transition model that is described and validated for JET data in [13] have been carried out. The simulations were done with a global model for the H-mode transition that follows the multi-machine scalings [14,15] for  $P_{\text{L-H}}$  and considers intermediate transitions to a type-III ELM regime. As can be seen in figure 9, the transition to stable high confinement is noticeably delayed compared to the simulations with prescribed density, even though a very high level of  $P_{\text{AUX}} = 73$  MW is applied. The results are sensitive to the scaling predictions, in fact, for the scaling with higher estimates for  $P_{\text{L-H}}$ , the H-mode cannot be maintained for lower levels of  $P_{\text{AUX}} \approx 40$  MW, as the plasma would return to type-III ELM My H-mode with degraded confinement reducing fusion power and triggering a back-transition to L-mode. It would follow that the  $Q = 10$  target may become difficult to achieve. On the other hand, an intermediate plasma regime would be advantageous for plasma control after the H-L transition, with an energy decay time that would get enhanced by an order of magnitude. The results are also sensitive to the density evolution: the particle content is predicted to increase rapidly after the L-H transition approaching the Greenwald density limit within the time scale of ETB formation. This result demonstrates that it may become difficult to control plasma density after the L-H transition.

**Conclusions.** According to simulation results, a slow ramp-up phase with late L-H transition gives the optimum fusion performance, whereas a fast ramp-up with early transition to high confinement is desirable in order to save  $V_s$  and extend the duration of the flat-top phase. Strong deterioration in predicted fusion output observed for high  $dI_{\text{pl}}/dt$  during ramp-up and/or early L-H transition can be attributed to a strong sensitivity of the anomalous transport model GLF-23 to  $s/q$ . A trade-off has to be established between the accumulation of resistive and sawtooth-induced  $V_s$  losses for small  $dI_{\text{pl}}/dt$  and limitations of the PF coil and fuelling systems for high  $dI_{\text{pl}}/dt$  for current ramp-down, with an optimum ramp-down period of  $\approx 200$ -250 s. A late transition to L-mode during current ramp-down seems to be feasible and advantageous for the extension of the ramp-down period. The compatibility of the H-L transition with the limitations and reaction times of the PF coil system can be ensured if the nominal distance from the plasma to the inner wall is increased, or if the energy reduction to L-mode conditions is slowed down, for example by an intermediate transition to type-III ELM regime. Shape control seems to be less problematic for the L-H transition, but in this case the details of the density evolution and fuelling as well as of the additional heating power (margins compared to  $P_{\text{L-H}}$ ) are critical in determining the successful evolution of the H-mode towards  $Q = 10$ .

## References

- [1] Albanese R., Mattei M., Calabro G., Villone F., ISEM 2003, Versailles, France.
- [2] Wiesen S. et al., JINTRAC-JET modelling suite, JET ITC-Report 2008.
- [3] Erba M. et al Plasma Phys. Control. Fusion 39 (1997) 261–276.
- [4] Waltz R.E. Phys. Plasmas 4 (1997) 2482.
- [5] Parail V. et al Nucl. Fusion 49 (2009) 075030.
- [6] Houlberg W.A. Nucl. Fus. 27 (1987) 1009–1020.
- [7] Chapman I.T. et al., "Sawtooth control in tokamak plasmas", this conference.
- [8] Mantica P. et al., Proc. 23rd IAEA Fusion Energy Conference (Daejon, Rep. of Korea) EXC/9-2.
- [9] Citrin J. et al., "Predictive transport analysis of JET and AUG hybrid scenarios", this conference.
- [10] Citrin J. et al. Nucl. Fusion 50 (2010) 115007.
- [11] Nunes I.M. et al., "ITER similarity current ramp-down experiments at JET", this conference.
- [12] Ambrosino G. et al., "Plasma position and shape control for ITER scenarios", EFDA Report 2008.
- [13] Belo P. et al, "Simulations of the H to L transition in JET plasmas", this conference.
- [14] Martin Y. R. et al. Journal of Physics: Conference Series 123 (2008) 012033.
- [15] Green B.J. et al. Plasma Phys. Control. Fusion 45 (2003) 687.

t [s]	$n_{e,\text{lin}}/n_{GW}$
1.3	0.4
80	0.4
130	0.85
500	0.85
530	0.8
550	0.6
723.3	0.6

Table 2 - Fraction of Greenwald density for the reference scenario.

t [s]	ECRH [MW] (off-axis)	ICRH [MW]	NBI [MW]
1.3-20	-	-	-
20-80	10	-	-
80-120	-	20	33
120-530	-	7	33
530-560	-	3	33
560-600	10	20	-
600-650	10	10	-
650-700	10	-	-
700-723.3	-	-	-

Table 1 – Auxiliary heating scheme for the reference scenario.

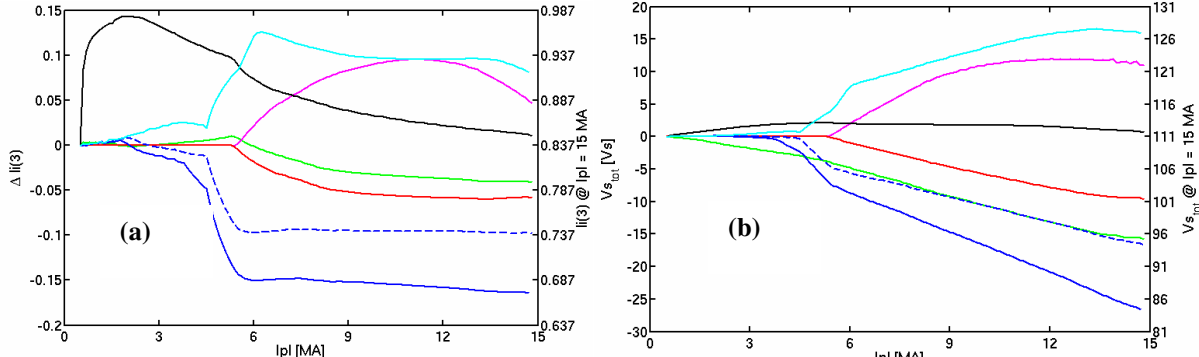


Figure 1 - deviation in  $li(3)$  (a) and total  $V_s$  consumption (b) during current ramp-up with respect to the reference case, for 20% of  $n_{GW}$  (green), 0 MW (magenta) and 20 MW (red) of ECRH, 30 eV of initial boundary temperature (black, reference case: 100 eV), -30% (cyan), +30% (blue dashed) and +66% of  $dI_{pl}/dt$  (blue solid).

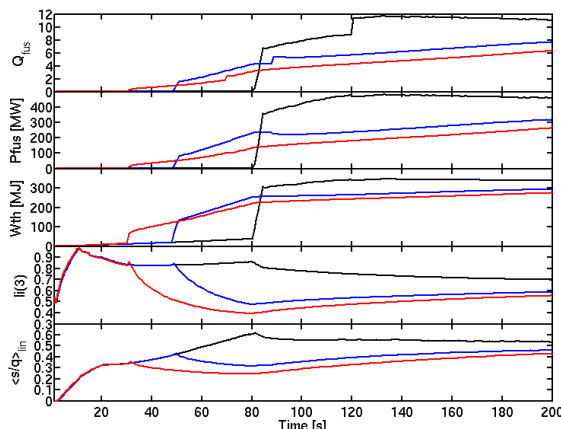


Figure 2 - from top to bottom: fusion  $Q$ ,  $P_{fus}$ ,  $W_{th}$ ,  $li(3)$  and line-averaged  $s/q$  ratio for the reference case with L-H transition at 15 MA (black colour), and two simulation cases with early L-H transition at 10 MA (blue colour) and 7 MA (red colour). In the latter case a Greenwald density fraction of 60% was applied to avoid the NB shine-through limit after the transition.

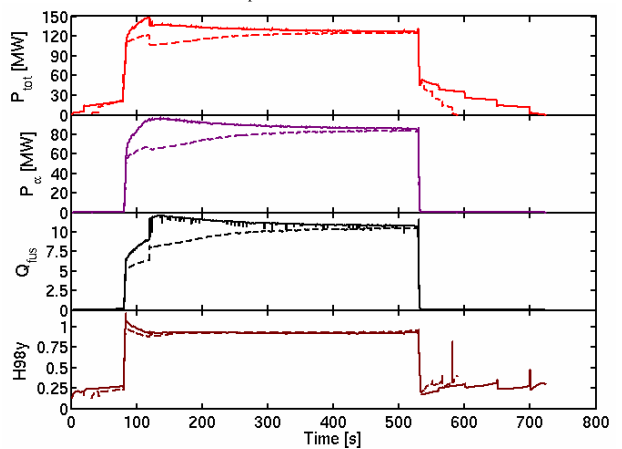


Figure 3 - total deposited heating power, alpha heat deposition, fusion  $Q$  and  $H98y$  (from top to bottom) for the complete reference scenario (solid) and the maximum ramp-rate scenario (dashed).

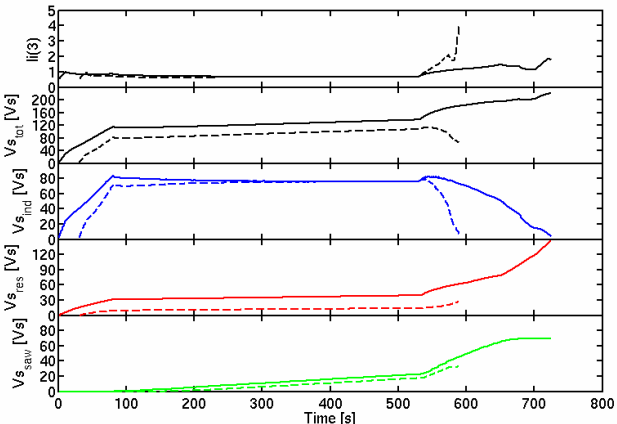


Figure 4 -  $I(3)$ , total, inductive, resistive and sawtooth-induced  $V_s$  consumption (from top to bottom) for the complete reference scenario (solid) and the maximum ramp-rate scenario (dashed).

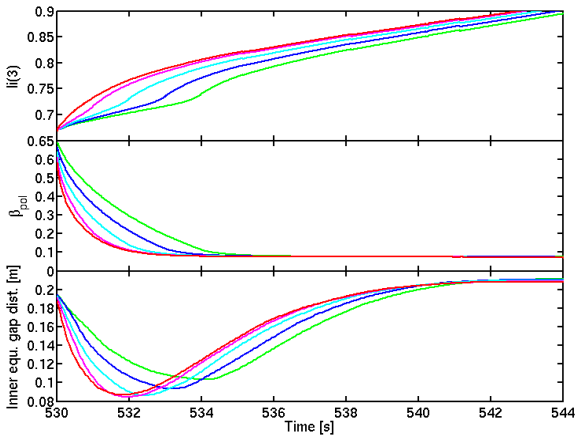


Figure 6 -  $I(3)$  (top), poloidal beta (middle) and equatorial distance between the separatrix and the inner wall (bottom), for a scan in the rapidity of the H-L transition for the reference scenario, red curves representing the most extreme case.

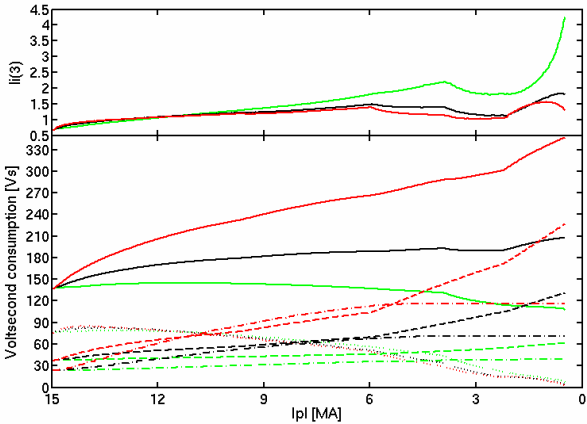


Figure 5 - top:  $I(3)$ , bottom: total (solid), inductive (dotted), resistive (dashed) and sawtooth-induced (dash-dotted)  $V_s$  consumption, for slow (red), medium (black, reference scenario) and fast ramp-down (green). The ramp-down periods are 400 s, 200 s and 60 s resp..

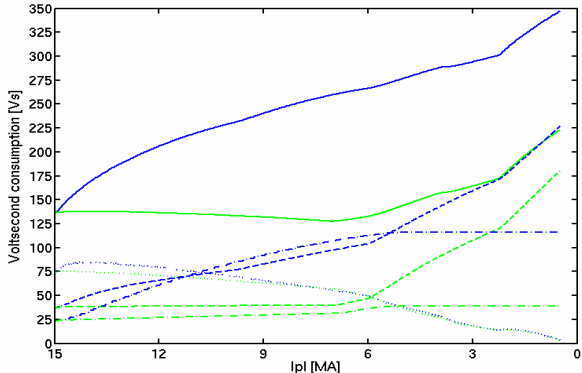


Figure 7 - total (solid), inductive (dotted), resistive (dashed) and sawtooth-induced (dash-dotted)  $V_s$  consumption for slow ramp-down (ramp-down period: 400 s) with H-L transition at 15 MA (blue) and at 7 MA (green).

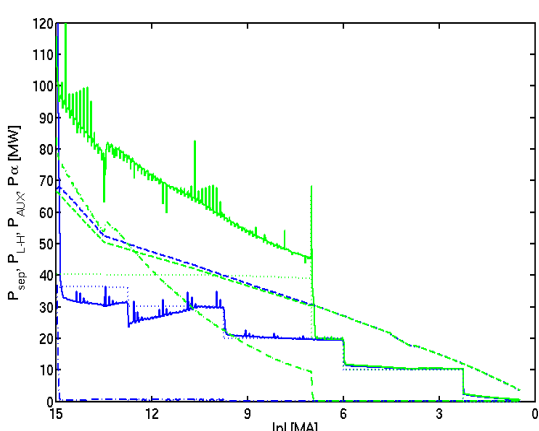


Figure 8 - power crossing the separatrix (solid), L-H transition power threshold [14] (dashed), auxiliary (dotted) and alpha heating power (dash-dotted), same simulation cases and colour scheme as for figure 7.

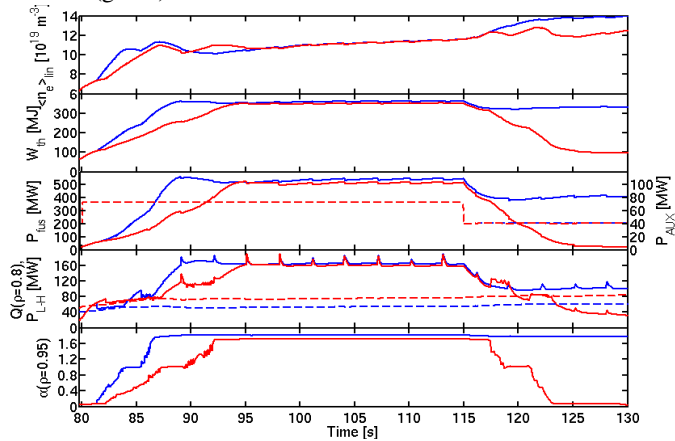


Figure 9 - from top to bottom: line-averaged electron density,  $W_{th}$ ,  $P_{fus}$  (solid) and  $P_{AUX}$  (dashed), total heat flux at  $\rho_{tor,norm.} = 0.8$  (solid) and  $P_{L-H}$  (dashed), normalised pressure gradient at  $\rho_{tor,norm.} = 0.95$ , for two fully predictive simulation cases with self-consistent L-H / H-L transition applying the  $P_{L-H}$  scalings in [14] (red) and [15] (blue).

**Acknowledgements:** This work has been funded with support from Fusion for Energy. This publication reflects the views only of the authors, and Fusion for Energy cannot be held responsible for any use which may be made of the information contained therein. Mario Cavinato, Yuri Gribov and Alberto Loarte are greatly acknowledged for helpful discussions, their advice and support to this work.